

# Instability of the layered orthorhombic post-perovskite phase of $\text{SrTiO}_3$ and other candidate orthorhombic phases under pressure

Churna Bhandari

Department of Physics and Astronomy, University of Missouri, Columbia, MO 65211 USA

Walter R. L. Lambrecht

Department of Physics, Case Western Reserve University, Cleveland, OH 44106-7079

While the tetragonal antiferro-electrically distorted (AFD) phase with space group  $I4/mcm$  is well known for  $\text{SrTiO}_3$  to occur below 105 K, there are also some hints in the literature of an orthorhombic phase, either at the lower temperature or at high pressure. A previously proposed orthorhombic layered structure of  $\text{SrTiO}_3$ , known as the post-perovskite or  $\text{CaIrO}_3$  structure with space group  $Cmcm$  is shown to have significantly higher energy than the cubic or tetragonal phase and to have its minimum volume at larger volume than cubic perovskite. The  $Cmcm$  structure is thus ruled out. We also study an alternative  $Pnma$  phase obtained by two octahedral rotations about different axes. This phase is found to have slightly lower energy than the  $I4/mcm$  phase in spite of the fact that its parent, in-phase tilted  $P4/mbm$  phase is not found to occur. Our calculated enthalpies of formation show that the  $I4/mcm$  phase occurs at slightly higher volume than the cubic phase and has a negative transition pressure relative to the cubic phase, which suggests that it does not correspond to the high-pressure tetragonal phase. The enthalpy of the  $Pnma$  phase is almost indistinguishable from the  $I4/mcm$  phase. Alternative ferro-electric tetragonal and orthorhombic structures previously suggested in literature are discussed.

## I. INTRODUCTION

The phase transitions in the perovskite material  $\text{SrTiO}_3$  (STO) have been studied extensively since the 1960s.<sup>1–5</sup> The perovskite structure is quite versatile and allows for several soft-phonon mode related phase transitions. While  $\text{BaTiO}_3$ , a classical ferroelectric (FE) undergoes a series of phase transitions in which the Ti atom is displaced inside its surrounding oxygen octahedron,  $\text{SrTiO}_3$  exhibits an anti-ferroelectric distortion (AFD) at 105 K consisting of a rotation of the  $\text{TiO}_6$  octahedra about one of the cubic axes. This leads to a tetragonal phase  $I4/mcm$ .<sup>6,7</sup> These two types of distortions are based on a soft-phonon instability at the zone center ( $\Gamma$ ) and at the  $R$ -point of the cubic Brillouin zone respectively. In the first-principles based Monte-Carlo simulations model allowing for both AFD and FE distortions and their coupling to strain, Zhong and Vanderbilt<sup>8</sup> predicted (at atmospheric pressure) a second transition at about 70 K to another tetragonal phase  $I4cm$  exhibiting both types of distortions and eventually at the lower temperature a transition to a monoclinic structure. Under pressure, an even more complex phase diagram was predicted by these simulations, including an orthorhombic phase and a rhombohedral phase. Experimentally, the lower temperature transitions have not been observed. The absence of these transitions is now well established to be due to the suppression of the transitions by quantum fluctuations.<sup>9–12</sup> The enormous increase in STO dielectric response below about 40 K has been associated with a quantum para-electric phase and possibly the existence of some new coherent quantum phase.<sup>10</sup> Early work by Lytle<sup>5</sup> hinted at an orthorhombic phase at the lower temperature but was neither confirmed nor the structure

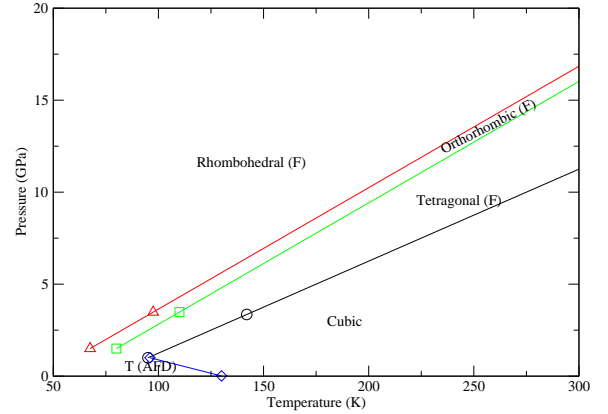


FIG. 1. (Color online) Extrapolated  $P - T$  phase diagram of  $\text{SrTiO}_3$ , the data points indicated by symbols are taken from Zhong and Vanderbilt<sup>8</sup> with their calculated pressures shifted from 5.5 to 0 GPa, the lines are extrapolations.

fully determined. On the other hand, as function of pressure, two transitions were observed, one at 5 GPa and a second at 14-15 GPa.<sup>13–16</sup> The first transition corresponds again to the transition from cubic to a tetragonal phase. However, it is not entirely clear whether this is the AFD  $I4/mcm$  or a FE phase. According to Zhong and Vanderbilt's calculations,<sup>8</sup> one would rather expect a FE phase with spacegroup  $P4mm$ . If one extrapolates their transition line between cubic and tetragonal FE, to higher pressures and temperatures, a transition to this phase is expected around 10 GPa at 300K followed by

a transition to an orthorhombic phase at slightly higher pressure as shown in Fig. 1. This is somewhat higher than the transition pressure observed of the cubic tetragonal transition but clearly this extrapolation is only very approximate. Their calculated pressure  $P = 5.4$  GPa corresponds to actual  $P=0$  GPa because of the LDA underestimate of the lattice constants but this shift is already included in Fig. 1.

The structure of the phase above 14 GPa has not yet been unambiguously determined either. Raman studies by Grzechnik *et al.*<sup>16</sup> suggested an orthorhombic phase. Cabaret *et al.* based on simulations of the X-ray absorption oxygen K-edge and fitted to measurements of the latter under pressure, suggested the orthorhombic  $\text{CaIrO}_3$  structure. This phase was further studied by Hachemi *et al.*<sup>17</sup>, reporting first-principles calculations of the elastic constants in each phase. However, they did not study the transition pressure or the total energy of this phase. Zhong and Vanderbilt<sup>8</sup> also mention an orthorhombic FE phase occurring in a narrow band between the tetragonal FE phase and the eventually rhombohedral FE phase occurring at high pressure and low temperature. This phase, however, is different from the  $\text{CaIrO}_3$  phase.

The structure suggested by Cabaret *et al.*<sup>15</sup> is the  $\text{CaIrO}_3$  structure, with spacegroup  $Cmcm$  ( $D_{2h}^{17}$ ) reported by Rodi and Babel.<sup>18</sup> This structure is also known as the post-perovskite structure and occurs for example in  $\text{MgSiO}_3$  under high-pressure in the earth's mantle.<sup>19</sup> Its structure is shown in Fig. 2. One can see that it is quite different from the perovskite structure, requiring significant re-bonding rather than simple soft-phonon mode distortions. It consists of 2D layers of edge-sharing octahedra intercalated with Sr ions. This is interesting from the point of view that from such layered structures, it may be possible to extract atomically thin 2D nanosheets by exfoliation, for example by inserting larger organic ions replacing the Sr atoms and thereby de-bonding the layers.

Motivated by the above interest in the possibility of a layered 2D post-perovskite orthorhombic structure of  $\text{SrTiO}_3$ , we here present a study of its stability relative to the known structures. Its electronic structure at the quasiparticle self-consistent  $GW$  level was already reported in a separate study.<sup>20</sup> As part of the present study, we also calculate the energy-volume relation in tetragonal and cubic perovskite structures.

Another possible route to an orthorhombic structure is considered. The AFD  $I4/mcm$  structure can be described as an out-of-phase rotation of successive  $\text{TiO}_6$  octahedra in the  $c$ -direction, where  $c$  is the 4-fold rotation axis. In other words, along these axes, the rotation is alternating clockwise and counter-clockwise. It belongs to the Glazer rotation system,  $a^0a^0c^-$ . We may alternatively consider the in-phase rotation  $a^0a^0c^+$ , which corresponds to the space group  $P4/mbm$  or a soft-phonon at the  $M$ -point. While it was previously found not to have an energy minimum at finite angle,<sup>21</sup> it may still be viewed as a starting point for further octahedral ro-

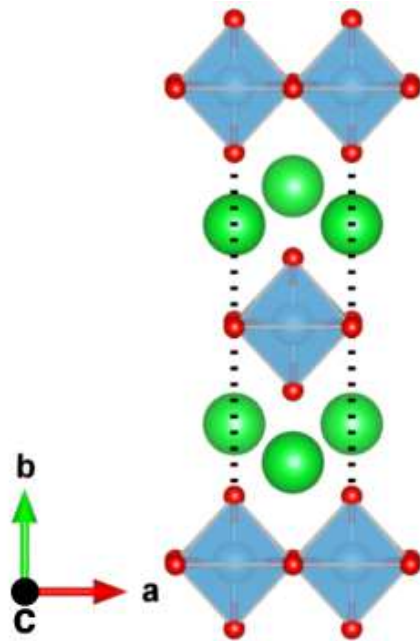


FIG. 2. Post-perovskite or  $\text{CaIrO}_3$  structure.

tations. From this tetragonal phase, we arrive at an orthorhombic phase  $Pnma$  by rotating about a second axis, with Glazer system  $a^+b^-b^-$ . This would be accompanied by motions of the Sr atoms as well. This phase occurs for example for  $\text{NaOsO}_3$ , where it is called the G-type as well as in halide perovskites, like  $\text{CsSnI}_3$ , where it is called the  $\gamma$ -phase.<sup>22</sup>

Recently, there has been renewed interest in  $\text{SrTiO}_3$  phase transitions because they also manifest themselves in transport properties at the two-dimensional electron gas formed between STO and  $\text{LaAlO}_3$  films grown on top of STO substrates. The study by Schoofs *et al.*<sup>23</sup> shows anomalies in transport at two temperatures and could also be taken as an indication of two phase transitions. However, this may also be related to thin film effects on the transition temperatures.

## II. METHOD

We used the density functional theory<sup>24</sup> as implemented in the Vienna *Ab initio* Simulation Package (VASP)<sup>25–27</sup> within the PBE exchange and correlation functional.<sup>28</sup> Additionally, the non-local correlation van der Waals vdW-DF functional is used which predicts the structural parameters of weakly interacting 2D layered materials more accurately compared to the local density (LDA) or generalized gradient approximations (GGA). There exist various versions of vdW-DF depending upon the choice of the exchange functional used.<sup>29–32</sup> In the present work we used the vdW-DF2<sup>33</sup> functional which is calculated within the semi-local exchange functional PW86 using the vdW-DF2 correlation kernel. For the

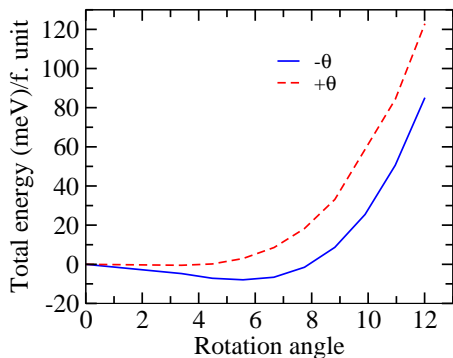


FIG. 3. (Color online) Total energy per formula unit as a function of octahedral rotation angle  $\theta$  with fully relaxed volume and  $c/a$  ratio for a given rotation angle. The dashed line corresponds to the in-phase rotation or  $P4/mbm$  structure, the solid line corresponds to the out-of-phase or  $I4/mcm$  structure. The total energy is minimum for  $\theta_{\min} = 5.57^\circ$  for the out of-phase  $I4/mcm$  phase.

Brillouin zone sampling, we used  $8 \times 8 \times 8$  for cubic,  $8 \times 8 \times 6$  for the tetragonal and orthorhombic structure respectively. The plane wave energy cut-off of 600 eV was enough for the convergence of plane wave basis-sets for all structures. The atomic positions were relaxed with the total energy converged with the precision of  $10^{-6}$  eV and the force converged with the precision of 5 meV/Å.

### III. RESULTS

#### A. Stability of STO under rotation

We first study the stability of STO under two types of AFD octahedral rotations: first the out of phase which occurs at low temperature and second the in-phase rotation which is a hypothetical structure. Fig. 3 shows the comparison of total energy per formula unit as a function of octahedral rotation angle  $\theta$ . Here  $+\theta$  corresponds to the rotation of adjacent octahedra in same direction along the  $c$ -axis while  $-\theta$  corresponds to the opposite. Fig. 3 shows no minimum for  $\theta \neq 0$  for the in-phase case. Nonetheless the minimum is very flat (it extends over a large range of angles between about  $\pm 5^\circ$ ) and indicates strong anharmonicity. On the other hand for the out of phase distortion, the total energy shows a global minimum at a finite rotation of  $\theta = 5.57^\circ$ . These results agree with the findings of Sai and Vanderbilt.<sup>21</sup>

#### B. Energy-volume and enthalpy *vs.* pressure

In this section, we discuss the stability of various phases under hydrostatic pressure. For more precise comparison, we used the van der Waals DFT which is known to predict more accurately the structural parameters for 2D like materials. In particular, the orthorhombic  $Cmcm$

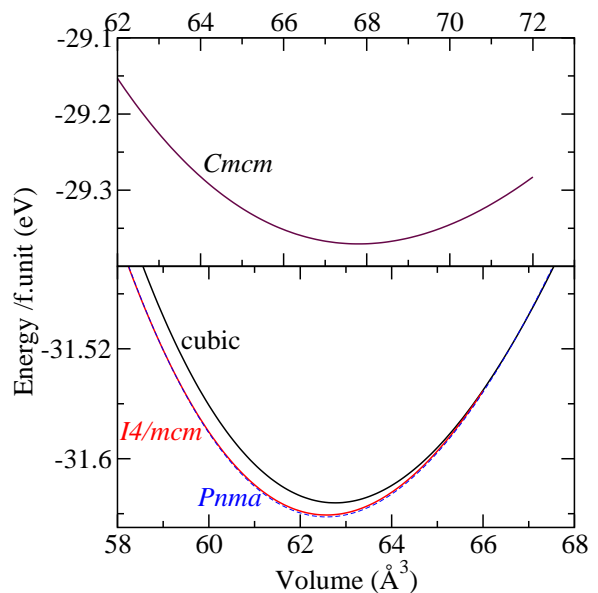


FIG. 4. (Color online) Pressure volume curve for cubic, tetragonal ( $I4/mcm$ ), orthorhombic ( $Cmcm$ ) and ( $Pnma$ ) structures with the PBE van der Waals functional obtained by fitting Murnaghan equation of state.

TABLE I. Computed (per formula unit) minimum volume ( $V_{\min}$ ), minimum energy ( $E_{\min}$ ), bulk modulus ( $B$ ) and derivative of bulk modulus ( $B'$ ) fitted using Murnaghan equation for all phases for pressure  $p = 0$  GPa and changes in volume ( $V$ ) at the critical pressure  $p_c$  for the cubic- $I4/mcm$  transition.

$p = 0$	Cubic	$Cmcm$	$I4/mcm$	$Pnma$
$\Delta E_{\min}$ (eV/f.u.)	0	2.260	-0.008	-0.010
$V_{\min}$ (Å <sup>3</sup> )	62.76	67.80	62.57	62.57
$B$ (GPa)	172.24	119.933	169.58	170.82
$B'$	4.405	4.170	4.32	4.45
$p_c = -6.4$				
$V$	65.22	-	65.06	-

structure has a 2D-layered character. Fig. 4 shows the total energy as a function of volume for four different crystal structures. The energy of the  $Cmcm$  structure is much higher than the other structures which already makes its existence rather implausible. The difference between the minima of the other phases and the  $Cmcm$  structure is 2.26 eV per formula unit. Secondly, its minimum volume occurs at higher volume near 68 Å<sup>3</sup>, compared to  $\sim 63$  Å<sup>3</sup> for the other phases. Thus it is not likely reached by high-pressure. We discuss this in more detail using the enthalpy *vs.* pressure calculations. On the other hand, the lower panel of Fig. 4 shows that the energy of the  $Pnma$  phase is very close to that of the tetragonal  $I4/mcm$  phase both being lower than the cubic phase. In fact, we find the  $Pnma$  phase to have the lowest energy but the energy difference is within the uncertainty of the calculations.

Table I shows the equilibrium volume, bulk modulus, the pressure derivative of the bulk modulus, and total energy difference relative to the cubic phase per formula unit. The total energy *vs.* volume is fitted by using the Murnaghan equation of state

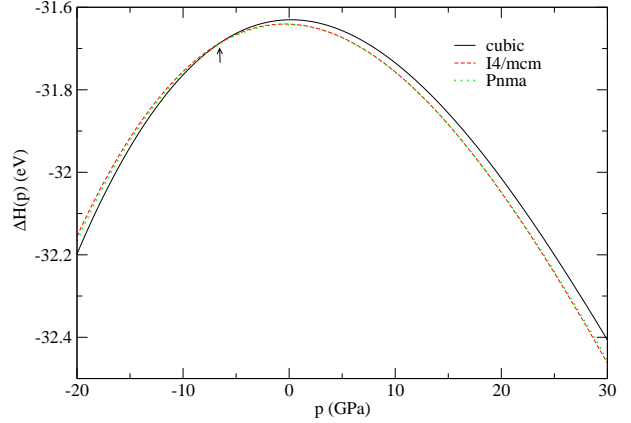
$$E(V) = E_0 + \frac{VB}{B'} \left( \frac{(V_0/V)^{B'}}{B' - 1} + 1 \right) - \frac{V_0 B}{(B' - 1)} \quad (1)$$

where  $E_0$ ,  $B$ ,  $B'$ , and  $V_0$  are the total energy, bulk modulus, derivative of bulk modulus, and volume at equilibrium. The calculated bulk modulus of the cubic structure is very close to the experimental value 174 GPa.<sup>34</sup> The bulk modulus of the  $I4/mcm$  and  $Pnma$  are close to that of the cubic structure, but for the orthorhombic  $Cmcm$  structure it is much smaller. The minimum volume obtained for  $p = 0$  GPa is lowest for the tetragonal  $I4/mcm$  and  $Pnma$  structures. This indicates that the transition pressure between cubic and the  $I4/mcm$  phase (or  $Pnma$ ) would occur at larger volume and thus negative pressure, as is confirmed by our enthalpy calculations, shown below. We also computed the volumes of the cubic and tetragonal structures at the critical pressure  $p_c = -6.4$  GPa. They occur at about  $65 \text{ \AA}^3$  with a change in volume of only 0.2 % between the two phases and close to the intersection of the two energy curves as can be seen in Fig. 4

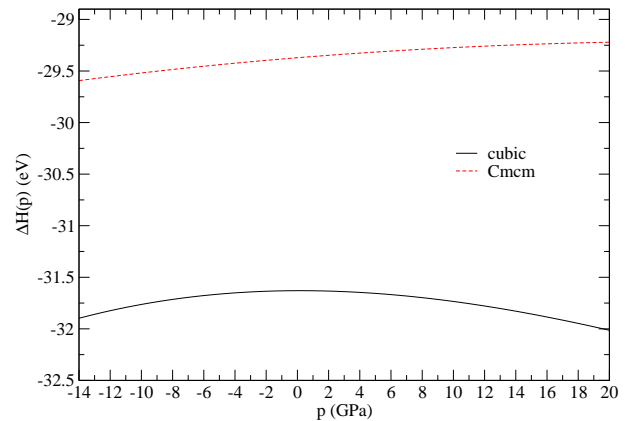
Next, in Fig. 5 we show the enthalpy changes  $\Delta H = E + p\Delta V$  for the various phases to determine the possible transition pressures given by intersections of the enthalpies. We use  $\Delta V = V - V_0$  with  $V_0$  the equilibrium volume of the cubic phase. This just subtracts the same  $pV_0$  term for all phases and allows to see their differences more clearly. We find that the cubic and  $I4/mcm$  phases have crossing enthalpies at  $p_t = -6.4$  GPa. The curve for the  $Pnma$  and  $I4/mcm$  are indistinguishable. However, for the cubic and  $Cmcm$  phases, there is clearly no possibility of a transition at all. This further rules out the possibility of the post-perovskite as high pressure phase.

#### IV. DISCUSSION AND CONCLUSIONS

In this paper, we have studied two candidate orthorhombic structures, the post-perovskite structure and a  $Pnma$  structure. We found the post-perovskite  $Cmcm$  structure, which has been suggested before in the literature to correspond to a high-pressure phase of  $\text{SrTiO}_3$  above 14 GPa, to be clearly unstable. It has a higher volume and much higher total energy than the cubic phase by about 2.26 eV/formula unit and no high-pressure transition to this phase is possible. So, this phase can definitely be ruled out. On the other hand, the  $Pnma$  phase corresponding to a double tilt of the octahedra about two axes and closely related to the in-phase single axis tetragonal tilted phase  $P4/mbm$  was found to have slightly lower energy than the known tetragonal  $I4/mcm$  phase in spite of the fact that an in-phase tetragonal tilt



(a)



(b)

FIG. 5. (Color online) Enthalpy as function of pressure for (a) cubic,  $I4/mcm$ ,  $Pnma$  (b) cubic and  $Cmcm$  phases.

$P4/mbm$  is not favored. The energy difference between the  $Pnma$  and the  $I4/mcm$  phase, however, is so small it may be considered to be within the error bar of the calculations. The transition pressure from the cubic phase to the  $I4/mcm$  phase was calculated to be  $-6.4$  GPa. The negative value indicates that a transition from cubic to  $I4/mcm$  is not a possible high-pressure transition. The tetragonal phase found under high pressure must thus be a different tetragonal phase than the one obtained at low temperature. This is consistent with a more complex temperature-phase diagram, as predicted by Zhong and Vanderbilt,<sup>8</sup> based on Monte Carlo simulations of an effective Hamiltonian model with degrees of freedom allowing for both ferro-electric and antiferro-electric in-

stabilities and parameters adjusted to density functional calculations. The latter suggests a different ferro-electric tetragonal phase  $P4mm$  is expected at room temperature and at pressures above 10 GPa pressure. None of the models thus far fully satisfactorily explains the sequence of the two observed pressure-induced phase transitions at room temperature. Unfortunately, a fully first-principles molecular dynamic simulation at finite temperature and pressure is beyond the scope of this work. Additional experimental work at determining the precise phases oc-

curing at high pressure appears to be needed to resolve the question.

## ACKNOWLEDGMENTS

This work was supported by the U.S. Air Force Office of Scientific Research under grant No. FA9550-18-1-0030.

- 
- <sup>1</sup> L. Rimai and G. A. deMars, Phys. Rev. **127**, 702 (1962).
  - <sup>2</sup> G. Rupprecht and R. O. Bell, Phys. Rev. **125**, 1915 (1962).
  - <sup>3</sup> R. O. Bell and G. Rupprecht, Phys. Rev. **129**, 90 (1963).
  - <sup>4</sup> H. P. R. Frederikse, W. R. Thurber, and W. R. Hosler, Phys. Rev. **134**, A442 (1964).
  - <sup>5</sup> F. W. Lytle, J. Appl. Phys. **35**, 2212 (1964).
  - <sup>6</sup> P. A. Fleury, J. F. Scott, and J. M. Worlock, Phys. Rev. Lett. **21**, 16 (1968).
  - <sup>7</sup> G. Shirane and Y. Yamada, Phys. Rev. **177**, 858 (1969).
  - <sup>8</sup> W. Zhong and D. Vanderbilt, Phys. Rev. Lett. **74**, 2587 (1995).
  - <sup>9</sup> K. A. Müller and H. Burkard, Phys. Rev. B **19**, 3593 (1979).
  - <sup>10</sup> K. A. Müller, W. Berlinger, and E. Tosatti, Zeitschrift für Physik B Condensed Matter **84**, 277 (1991).
  - <sup>11</sup> R. Viana, P. Lunkenheimer, J. Hemberger, R. Böhmer, and A. Loidl, Phys. Rev. B **50**, 601 (1994).
  - <sup>12</sup> W. Zhong and D. Vanderbilt, Phys. Rev. B **53**, 5047 (1996).
  - <sup>13</sup> T. Ishidate, S. Sasaki, and K. Inoue, High Pressure Research **1**, 53 (1988), <http://dx.doi.org/10.1080/08957958808202480>.
  - <sup>14</sup> T. Ishidate and T. Isonuma, Ferroelectrics **137**, 45 (1992), <http://dx.doi.org/10.1080/00150199208015936>.
  - <sup>15</sup> D. Cabaret, B. Couzinet, A. Flank, J. Iti, P. Lagarde, and A. Polian, AIP Conference Proceedings **882**, 120 (2007).
  - <sup>16</sup> A. Grzechnik, G. H. Wolf, and P. F. McMillan, Journal of Raman Spectroscopy **28**, 885 (1997).
  - <sup>17</sup> A. Hachemi, H. Hachemi, A. Ferhat-Hamida, and L. Louail, Physica Scripta **82**, 025602 (2010).
  - <sup>18</sup> F. Rodi and D. Babel, Zeitschrift für anorganische und allgemeine Chemie **336**, 17 (1965).
  - <sup>19</sup> M. Murakami, K. Hirose, K. Kawamura, N. Sata, and Y. Ohishi, Science **304**, 855 (2004), <http://science.sciencemag.org/content>.
  - <sup>20</sup> C. Bhandari, M. van Schilgaarde, T. Kotani, and W. R. L. Lambrecht, Phys. Rev. Materials **2**, 013807 (2018), <https://doi.org/10.1103/PhysRevMaterials.2.013807>.
  - <sup>21</sup> N. Sai and D. Vanderbilt, Phys. Rev. B **62**, 13942 (2000).
  - <sup>22</sup> L.-y. Huang and W. R. L. Lambrecht, Phys. Rev. B **90**, 195201 (2014).
  - <sup>23</sup> F. Schoofs, M. Egilmez, T. Fix, J. L. MacManus-Driscoll, and M. G. Blamire, Applied Physics Letters **100**, 081601 (2012), <http://dx.doi.org/10.1063/1.3687706>.
  - <sup>24</sup> W. Kohn and L. J. Sham, Phys. Rev. **140**, A1133 (1965).
  - <sup>25</sup> G. Kresse and J. Hafner, Phys. Rev. B **47**, 558 (1993).
  - <sup>26</sup> G. Kresse and J. Furthmüller, Phys. Rev. B **54**, 11169 (1996).
  - <sup>27</sup> G. Kresse and D. Joubert, Phys. Rev. B **59**, 1758 (1999).
  - <sup>28</sup> J. P. Perdew and W. Yue, Phys. Rev. B **33**, 8800 (1986).
  - <sup>29</sup> M. Dion, H. Rydberg, E. Schröder, D. C. Langreth, and B. I. Lundqvist, Phys. Rev. Lett. **92**, 246401 (2004).
  - <sup>30</sup> G. Román-Pérez and J. M. Soler, Phys. Rev. Lett. **103**, 096102 (2009).
  - <sup>31</sup> J. Klimeš, D. R. Bowler, and A. Michaelides, Journal of Physics: Condensed Matter **22**, 022201 (2010).
  - <sup>32</sup> J. c. v. Klimeš, D. R. Bowler, and A. Michaelides, Phys. Rev. B **83**, 195131 (2011).
  - <sup>33</sup> K. Lee, E. D. Murray, L. Kong, B. I. Lundqvist, and D. C. Langreth, Phys. Rev. B **82**, 081101 (2010).
  - <sup>34</sup> R. O. Bell and G. Rupprecht, Phys. Rev. **129**, 90 (1963).